JOURNAL OF MODERN OPTICS, 1996, VOL. 43, NO. 2, 417–432

Coherent states in finite-dimensional Hilbert space and their Wigner representation

TOMÁŠ OPATRNÝ

Department of Theor. Physics, Palacký University, Svobody 26, 771 46 Olomouc, Czech Republic

ADAM MIRANOWICZ

Nonlinear Optics Division, Institute of Physics, Adam Mickiewicz University, 60-780 Poznań, Poland

and JIŘÍ BAJER

Laboratory of Quantum Optics, Palacký University, 17 listopadu 50, 772 07 Olomouc, Czech Republic

(*Received 14 March 1995; revision received 13 June 1995*)

Abstract. We consider two definitions of coherent states in a finite-dimensional Hilbert space based on (i) truncation of the usual coherent state expansion and (ii) generalization of the displacement operator acting on vacuum. The number-phase Wigner function is computed for such states. Analytical results and numerically computed graphs are presented. Special attention is paid to two-level states and to their Stokes parameter representations.

1. Introduction

The most common states in quantum optics are Glauber coherent states (CS). In the past three decades progress in the field of coherent states, including their generalizations and applications, has been truly breathtaking [1]. Quite recently, generalizations of coherent states comprising the finite-dimensional case have attracted some interest due to popularity of the Pegg–Barnett Hermitian phase operator [2] defined in a finite-dimensional Hilbert space (FDHS).

There are several reasons for studying states in such spaces. Firstly, it gives us a deeper insight into the Pegg–Barnett formalism [2] of the Hermitian optical phase operator constructed in a finite $(s + 1)$-dimensional Hilbert space. The key idea of the Pegg–Barnett procedure is to calculate all the physical quantities such as expectation values of variances in the finite-dimensional space and only then to take the limit $s \to \infty$. Bužek *et al.* [3] have pointed out that all quantities (in particular states) analysed within the Pegg–Barnett formalism, should be properly defined in the same $(s + 1)$-dimensional state space before finally going over to the infinite limit. So it is useful for a better understanding of the Pegg–Barnett formalism to construct finite-dimensional states and to know what exactly is happening before the limit is taken. Secondly, we can treat these states as states of a real one-mode electromagnetic field which fulfil the condition of truncated Fock expansion. These states can in principle be generated using methods described by Vogel *et al.* [4], Garraway *et al.* [5] or Leoński and Tanaś [6].

0950–0340/96 $12·00

Thirdly, the obtained results are also applicable to other systems described by the FDHS model, like spin systems or systems of two-level atoms. In such cases we should talk, for example, about the z-component of the spin and its azimuthal orientation rather than about the photon number and phase. However, the states studied here were first discussed in quantum optical papers and we shall also keep the terminology of quantum optics.

It is possible to define FDHS coherent states in several ways. We can do this using the concept of Lie group representations (see, e.g. [7]), or postulating the validity of some properties of the infinite-dimensional Hilbert space (IDHS) CS for the finite-dimensional CS. In this paper we shall be interested in two definitions of the latter case. First, coherent states in an FDHS are usually treated as the displaced vacuum, where the displacement operator is defined in an analogous way to the IDHS (the Glauber treatment of CS [8]). This idea was applied in the work of Bužek and co-workers [3] and further studied by Miranowicz *et al.* [9]. Here, we shall refer to these states as *finite-dimensional Glauber coherent states* or simply *coherent states* in an FDHS. Another definition is based on the postulate that the Fock expansion of the finite-dimensional CS shall be equal to the truncated expansion of the usual infinite-dimensional CS. This approach was extensively developed by Kuang *et al.* [10] and here we shall refer to states of this kind as *truncated coherent states* in an FDHS. These two constructions were used in the analysis of other finite-dimensional states [11].

Although many properties of such states are known by now, for their better understanding it is very useful to analyse graphs of their quasi-distributions. The main aim of this paper, apart from the explicit comparison of different coherent states in an FDHS, is to discuss their finite-dimensional Wigner functions. Our treatment is based mostly on the work of Wootters [12] and Vaccaro and Pegg [13]. After recalling the most important general properties of the Wigner functions in section 2, we present some analytical results and graphs of the Wigner functions for several types of finite-dimensional state in section 3.

The simplest non-trivial case of the FDHS is the Hilbert space of the two-level system. This model provides a highly useful tool in many branches of physics, and states of this system have often been studied. Here, in section 4, we present the properties of these states from other points of view, using Stokes parameter representations and calculating the respective Wigner function.

2. Wigner function

A very interesting way of treating quantum states of simple systems is to use quasi-distributions. The most popular of the latter is the Wigner function (W-function) [14], which has the classical-like property that some of its marginal integrals are equal to actual distributions of physical quantities (it can, however, take negative values in contrast to classical distributions).

Wigner's definition of the function of continuous variables has been generalized to the case of finite-state systems by Wootters [12]. The problem of introducing the Wigner function with discrete spin variables was analysed even earlier [15]. Wootters' definition borrows much from these studies; however, contrary to the former approaches, it is applicable to arbitrary-dimensional state space and is defined on an explicitly geometrical phase space. We use the Wootters definition of the W-function [12] which was also applied by Vaccaro and Pegg [13].

Wootters' idea is based on the assumption that the Hilbert space of the system

is spanned by $(s+1)$ eigenvectors $|v_i\rangle$ of a quantity v and equivalently by $(s+1)$ eigenvectors $|w_j\rangle$ of a quantity w, where these quantities are mutually independent (see also [16]). This means that the absolute value of the scalar product $|\langle v_i|w_j\rangle|$ is a constant, independent of the indices i, j. As can be checked, in the case of the finite-dimensional harmonic oscillator the eigenvectors of the quadratures $\hat{X} = (\hat{a} + \hat{a}^\dagger)/2$ and $\hat{Y} = (\hat{a} - \hat{a}^\dagger)/2i$ (commonly used as continuous arguments of the infinite-dimensional harmonic oscillator W-functions) do not fulfil this condition. Instead, a proper pair of mutually independent quantities is here provided by the photon number n and the phase θ, whose operator is defined by [2]

$$\hat{\Phi}_\theta = \sum_{m=0}^{s} \theta_m |\theta_m\rangle\langle\theta_m|, \tag{1}$$

where the $|\theta_m\rangle$ are the phase states:

$$|\theta_m\rangle = (s+1)^{-1/2} \sum_{n=0}^{s} \exp(in\theta_m)|n\rangle, \tag{2}$$

with $\theta_m = \theta_0 + 2\pi m/(s+1)$. Here, θ_0 is the initial reference phase and $(s+1)$ is the dimension of the Hilbert space $\mathscr{H}^{(s)}$. Wigner functions for phase and number were first studied by Vaccaro and Pegg [13] for the limit of very high s. Let us mention that new interesting definitions of W-functions in n and θ have been proposed recently by Lukš and Peřinová [17] and Vaccaro [18]. In this paper we analyse the W-function in the arguments n and θ_m, but do not restrict our considerations to high-dimensional Hilbert spaces (we consider even the case of $s = 1$).

Let us recall some main features of Wootters' definition of the W-function for the finite-dimensional harmonic oscillator. The W-function value of the 'phase space point' (n, θ_m) is proportional to the mean value of the phase space point operator $\hat{A}(n, m)$ which for prime (see remark [19]) numbers $s + 1 \geqslant 3$ is [13]:

$$\hat{A}(n, m) = \sum_{p=0}^{s} \exp[-4i\pi np/(s+1)]|\theta_{m+p}\rangle\langle\theta_{m-p}| \tag{3}$$

and for $s + 1 = 2$ is given by [12]:

$$\hat{A}(n, m) = (1/2)[(-1)^n\hat{\sigma}_z + (-1)^m\hat{\sigma}_x + (-1)^{n+m}\hat{\sigma}_y + \hat{1}], \tag{4}$$

where $\hat{\sigma}_j$ are the Pauli matrices. The Wigner function is then

$$W(n, \theta_m) = (s+1)^{-1}\langle\hat{A}(n, m)\rangle. \tag{5}$$

Vice versa, with the W-function available for a given state, one finds its density operator by inversion of equation (5):

$$\hat{\rho} = \sum_{m,n} W(n, \theta_m)\hat{A}(n, m). \tag{6}$$

The situation becomes more highly complicated for composite numbers $(s+1)$, where the phase space point operator is constructed as the direct product of prime-number-dimensional phase space point operators. Here, for simplicity, we consider only the case of prime numbers $(s+1)$. For pure states, which can be written in the Fock basis

$$|\psi\rangle(s) = \sum_{n=0}^{s} C_n|n\rangle \equiv \sum_{n=0}^{s} b_n^{(s)} \exp(i\varphi_n|n\rangle, \tag{7}$$

the Wigner function can be expressed in terms of the complex decomposition coefficients C_n [13]:

$$W(n, \theta_m) = (s+1)^{-1} \sum_{k=0}^{M} C_k^* C_{M-k} \exp\left[\mathrm{i}(2k - M)\theta_m\right] + (s+1)^{-1} \sum_{k=M+1}^{s} C_k^* C_{M-k+s+1} \exp\left[\mathrm{i}(2k - M - s - 1)\theta_m\right], \quad (8)$$

where $M \equiv 2n \bmod (s+1)$.

In infinite-dimensional Hilbert space, where the W-function arguments are continuous (quadratures X, Y), a marginal integral along any straight line $aX + bY + c = 0$ is non-negative and can be considered to be the probability. A similar situation arises in the finite-dimensional case: we can define lines as sets of discrete points (n, θ_m) for which the relation $(an + bm + c) \bmod N = 0$ holds (a, b, c are integers here). Again, sums of the discrete W-function values on such sets are non-negative. The mod $(s+1)$ relations are essential here and are connected to some periodic properties of the discrete W-function—the maximum value of each argument (m or n) is topologically followed by its minimum (zero in our case). This means that the discrete W-function is defined on a torus (or more precisely on a discrete set of points of a torus). The 'lines' are then points of closed toroidal spirals or, in a special case, points of a circle. The periodic property is quite natural for the phase index m, but may seem strange for the problem number n. In the next section we shall draw attention to some consequences of the periodicity in n for different coherent states.

One of the aims of this paper is to show graphs of the discrete W-functions for finite-dimensional coherent states. Because of the discreteness of the arguments, the W-function graph should be a histogram. Two-dimensional projections of such three-dimensional histograms would be very confusing; therefore, for better legibility of the graphs we decided to depict them topographically. The darker a region, the higher is the value of the W-function it represents. Moreover, negative values of the W-function are marked by crosses. As mentioned above, the most natural way of presenting finite-dimensional W-function graphs is to construct them on tori. Two such graphs for vacuum and coherent state are shown in figure 1. Nevertheless, because the present paper is printed on two-dimensional sheets, it is better to use two-dimensional objects as a compromise. In what follows we shall work with circular graphs. Here, the periodicity in phase is very apparent: however, one should keep in mind that some consequences of the periodicity in n can appear,

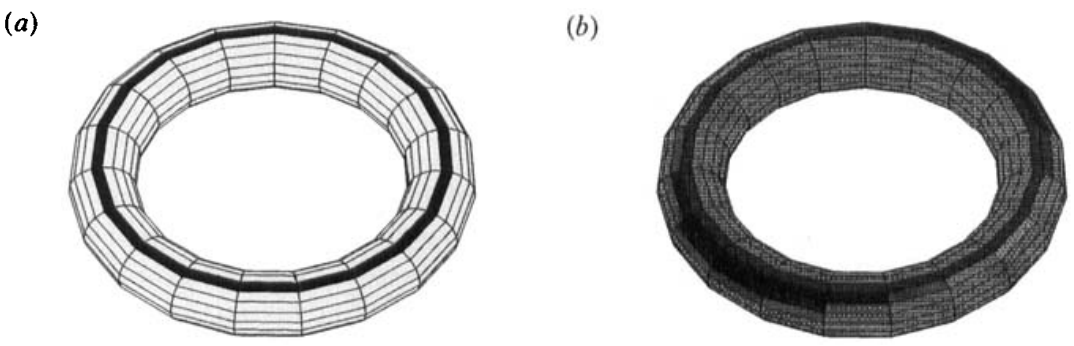

Figure 1. Wigner function on a torus in $\mathcal{H}^{(s)}$ with $s = 18$ for $\alpha = T = 8{\cdot}8$: (*a*) a Glauber coherent state $|\alpha\rangle_{(s)}$, (20) which is almost vacuum; (*b*) a truncated coherent state $|\tilde{\alpha}\rangle_{(s)}$, (20). The darker a region, the higher is the value of the W-function.

e.g. some peak can be located partially at the outer boundary of the circle ($n \approx s$) and can 'continue' near the centre ($n \approx 0$). In the next section W-functions of different finite-dimensional coherent states will be presented. For a better understanding of their meaning, let us recall their close correspondence to the photon number distribution and to the phase distribution. The sum of the W-function values, with constant n, over all arguments θ_m (i.e. 'along a circle') gives the probability of n photons and similarly the sum, at constant θ_m, over all n values (i.e. 'along a radius') gives the probability of the phase θ_m—at least in systems that are fully described by finite-number state models. However, if we want to interpret our results as describing states of a usual one-mode field under the condition that all Fock $|n\rangle$ components with $n > s$ are absent, then the real phase probability distribution is obviously continuous. Let us here briefly discuss its connection to the obtained discrete distribution. If s is greater than or equal to the largest Fock state component of a given state, which by definition is our case, then the discrete probabilities (from the discrete Wigner phase marginal) are proportional to the values of the continuous phase probability distribution in the discrete set of points $\theta_m = [2\pi(s+1)]m + \theta_0$. Nevertheless, we could easily obtain the other values also, even though not directly. We could use a finite-dimensional version of the sampling theorem—if the n-distribution is limited, then to describe a state in the phase representation only a discrete set of phase amplitudes is necessary. Anyway, it is clear that the $(s+1)^2$ real values of the discrete W-function yield the same information as the $(s+1)^2$ real non-zero parameters of the related density matrix. The discrete phase distribution (i.e. the discrete Wigner phase marginal) for a finite-dimensional coherent state and the continuous Pegg–Barnett phase probability distribution for an ordinary coherent state were compared in detail by Miranowicz *et al.* [9].

3. Finite-dimensional states and their Wigner functions

3.1. *Truncated coherent states in FDHS*

Kuang *et al.* [10] defined the normalized finite-dimensional CS truncating the Fock base expansion of the Glauber infinite-dimensional CS, $|\alpha\rangle_{(\infty)}$, or equivalently by the action of the operator $\exp(\bar{\alpha}\hat{a}^\dagger)$ (with proper normalization) on the vacuum state. We shall pay some attention to the Kuang *et al.* approach because it is the most similar to the Vaccaro–Pegg treatment [13] of the coherent states Wigner function. The states $|\bar{\alpha}\rangle_{(s)}$, where $\bar{\alpha} = |\bar{\alpha}| \exp(i\varphi)$, can be defined as follows in the Fock expansion [10]:

$$|\bar{\alpha}\rangle_{(s)} = \mathcal{N}^{(s)} \exp(\bar{\alpha}\hat{a}^\dagger)|0\rangle = \sum_{n=0}^{s} \exp(in\varphi) b_n^{(s)} |n\rangle, \tag{9}$$

where

$$b_n^{(s)} = \mathcal{N}^{(s)} |\bar{\alpha}|^n (n!)^{-1/2}. \tag{10}$$

Here, we rewrite the normalization constant in the form

$$\mathcal{N}^{(s)} = \left(\sum_{n=0}^{s} \frac{|\bar{\alpha}|^{2n}}{n!} \right)^{-1/2} = \left\{ (-1)^s L_s^{-s-1}(|\bar{\alpha}|^2) \right\}^{-1/2} \tag{11}$$

in terms of generalized Laguerre polynomials $L_s^n(x)$. For future reference, we shall use the concept of *truncated coherent states* for the states $|\bar{\alpha}\rangle_{(s)}$ defined by (9). Let

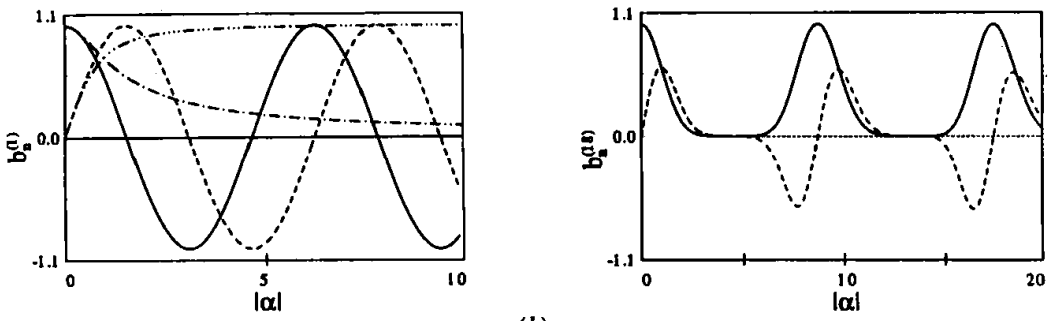

(*a*) (*b*)

Figure 2. The superposition coefficients $b_{0,1}^{(s)}$ as a function of the parameter $|\alpha| = |\bar{\alpha}|$ for Glauber coherent states $|\alpha\rangle_{(s)}$, (21), and truncated coherent states $|\bar{\alpha}\rangle_{(s)}$, (10), in finite-dimensional Hilbert spaces: (*a*) $\mathscr{H}^{(1)}$ and (*b*) $\mathscr{H}^{(18)}$; $b_0^{(s)}$ for $|\alpha\rangle_{(s)}$—solid lines, $b_1^{(s)}$ for $|\alpha\rangle_{(s)}$—dashed lines, $b_0^{(s)}$ for $|\bar{\alpha}\rangle_{(s)}$—dot-dashed lines, $b_1^{(s)}$ for $|\bar{\alpha}\rangle_{(s)}$—dot-dot-dashed lines.

us note that the normalization constant $\mathscr{N}^{(s)}$, (11), can readily be expressed in a compact form using generalized Laguerre polynomials (or, equivalently, incomplete gamma functions, etc.) without the necessity of introducing any extra functions as, for example, the one in [10]. In figure 2, the superposition coefficients $b_{0,1}^{(s)}$, (10), of the truncated coherent states $|\bar{\alpha}\rangle_{(s)}$ are presented as a function of the parameter $|\bar{\alpha}| \equiv |\alpha|$ in the finite-dimensional Hilbert spaces $\mathscr{H}^{(1)}$ and $\mathscr{H}^{(18)}$. We stress that the coefficients $b_n^{(s)}$, (10), are aperiodic functions of $|\bar{\alpha}|$.

By definition, the truncated coherent states $|\bar{\alpha}\rangle_{(s)}$, (9), go over into the usual (i.e. infinite-dimensional) Glauber coherent states $|\alpha\rangle_{(\infty)}$ in the limit $s \to \infty$. Nevertheless, for better comparison with the finite-dimensional Glauber coherent states $|\alpha\rangle_{(s)}$, we show this property explicitly by expanding the scalar products between $|\bar{\alpha}\rangle_{(s)}$ and $|\alpha\rangle_{(\infty)}$ in a series of $|\alpha|$. We have

$$_{(\infty)}\langle\alpha|\bar{\alpha}\rangle_{(1)} = 1 - |\alpha|^4/4 + |\alpha|^6/6 - \mathcal{O}(|\alpha|^8), \tag{12}$$

$$_{(\infty)}\langle\alpha|\bar{\alpha}\rangle_{(2)} = 1 - |\alpha|^6/12 + |\alpha|^8/16 - \mathcal{O}(|\alpha|^{10}), \tag{13}$$

$$_{(\infty)}\langle\alpha|\bar{\alpha}\rangle_{(3)} = 1 - |\alpha|^8/48 + |\alpha|^{10}/60 - \mathcal{O}(|\alpha|^{12}), \tag{14}$$

where we assume that $\alpha = \bar{\alpha}$. We have found that with increasing dimension $(s + 1)$,

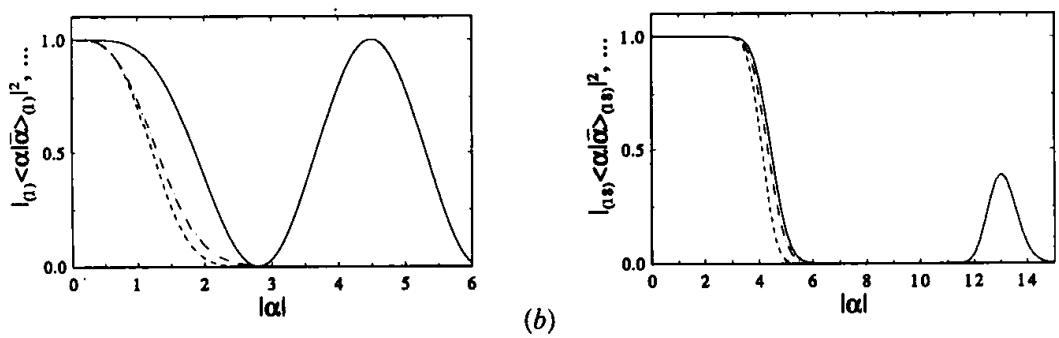

(*a*) (*b*)

Figure 3. The dependence on $|\alpha| \equiv |\bar{\alpha}|$ of the squared scalar products between the finite-dimensional Glauber coherent states $|\alpha\rangle_{(s)}$, (20), and truncated coherent states $|\bar{\alpha}\rangle_{(s)}$, (9), and the usual (i.e. infinite-dimensional) Glauber coherent states $|\alpha\rangle_{(\infty)}$ for (*a*) $s = 1$ and (*b*) $s = 18$: $|_{(s)}\langle\alpha|\bar{\alpha}\rangle_{(s)}|^2$—solid lines; $|_{(\infty)}\langle\alpha|\alpha\rangle_{(s)}|^2$—dashed lines; $|_{(\infty)}\langle\alpha|\bar{\alpha}\rangle_{(s)}|$—dash–dotted lines.

the truncated CS $|\bar{\alpha}\rangle_{(s)}$ approach the usual CS $|\alpha\rangle_{(\infty)}$ in a form

$$ {}_{(\infty)}\langle\alpha|\bar{\alpha}\rangle_{(s)} = 1 - \frac{|\alpha|^{2(s+1)}}{2(s+1)!} + \mathcal{O}(|\alpha|^{2(s+2)}). \tag{15} $$

In figure 3, among other functions, we have depicted squared scalar products $|{}_{(\infty)}\langle\alpha|\bar{\alpha}\rangle_{(s)}|^2$ between the usual Glauber coherent states $|\alpha\rangle_{(\infty)}$ and truncated coherent states $|\bar{\alpha}\rangle_{(s)}$, (9), as a function of the parameter $|\alpha|$ for two cases of $s = 1$ and $s = 18$. The higher the s, the greater is the range of $|\alpha|$ where the scalar product tends to unity. It is clearly seen that for $|\alpha|^2 \ll s$, the states $|\alpha\rangle_{(s)}$ and $|\bar{\alpha}\rangle_{(s)}$ approach each other. However, for values $|\alpha|^2 \approx s$ or greater than s, the differences between the states become essential.

Substituting expression (7) into equation (8) we get

$$ W(n, \theta_m) = \frac{\mathcal{N}^2}{s+1} \sum_{k=0}^{M} \frac{|\bar{\alpha}|^M}{[k!(M-k)!]^{1/2}} \exp[i(2k - M)(\theta_m - \varphi)] $$
$$ + \frac{\mathcal{N}^2}{s+1} \sum_{k=M+1}^{s} \frac{|\bar{\alpha}|^{M+s+1}}{[k!(M-k+s+1)!]^{1/2}}, \tag{16} $$

where $M = 2n \bmod (s+1)$ and, for simplicity, we drop the superscript in the normalization constant. Equation (16) can be written in a form providing for a simple comparison with the Vaccaro–Pegg result:

$$ W(n, \theta_m) = (s+1)^{-1} \Lambda_1(n, |\bar{\alpha}|) \Phi_1(n, \theta_m, \varphi) + (s+1)^{-1} \Lambda_2(n, |\bar{\alpha}|) \Phi_2(n, \theta_m, \varphi), \tag{17} $$

where

$$ \Lambda_1(n, |\bar{\alpha}|) = \mathcal{N}^2 |\bar{\alpha}|^M / l!, $$
$$ \Phi_1(n, \theta_m, \varphi) = l! \sum_{k=0}^{M} \frac{\cos[(2k - M)(\theta_m - \varphi)]}{[k!(M-k)!]^{1/2}} \tag{18} $$

and

$$ \Lambda_2(n, |\bar{\alpha}|) = \mathcal{N}^2 |\bar{\alpha}|^{M+s+1} / t!, $$
$$ \Phi_2(n, \theta_m, \varphi) = t! \sum_{k=M+1}^{s} \frac{\cos[(2k - M - s - 1)(\theta_m - \varphi)]}{[k!(M-k+s+1)!]^{1/2}}. \tag{19} $$

Here, $l = [\![M/2]\!]$ is the largest integer not exceeding $M/2$, and similarly $t = [\![(M+1+s)/2]\!]$. We note that the functions Λ_i do not depend upon the phase φ of $\bar{\alpha}$ and similarly the functions Φ_i do not depend upon its amplitude $|\bar{\alpha}|$. In the Vaccaro–Pegg treatment, $|\bar{\alpha}|^2$ was always much less than s, so that the second term of equation (17) could be neglected. Then the Wigner function was factorizable into the amplitude-dependent function Λ_1 and the phase-dependent function Φ_1, the normalizing constant $\mathcal{N}^{(s)}$ being approximated by $\exp(-|\bar{\alpha}|^2/2)$. It can be seen that for general values of $\bar{\alpha}$ of the truncated coherent states this factorization is no longer feasible. Moreover, for too large $|\bar{\alpha}|$, the second term of equation (17) becomes predominant. We compare the different shapes of the W-functions for various $\bar{\alpha}$ in figure 4. The functions are computed for $s = 18$. We find that for small $|\bar{\alpha}|$ the shape is essentially the same as in [13]: for $n \leqslant s/2$ there are two peaks for opposite phases, whereas for $n > s/2$ we observe a peak and an anti-peak. The peaks or anti-peaks are located at such positions that on summing the W-function with constant n (or θ_m) over θ_m (or n), we get the probability distribution of n (or

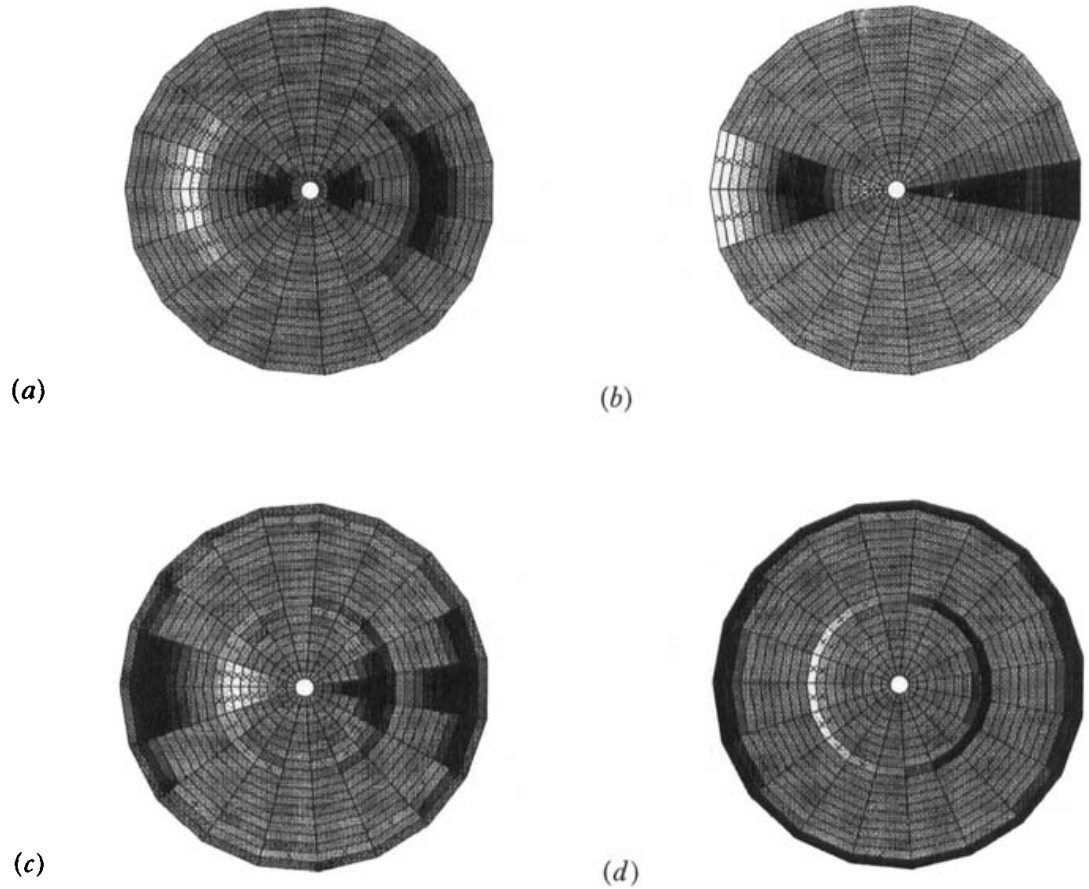

Figure 4. Wigner function of truncated coherent states $|\bar{\alpha}\rangle_{(s)}$, (9), for $s = 18$, $\bar{\alpha} = |\bar{\alpha}| \exp(i\varphi)$, $\varphi = 0$: (*a*) $|\bar{\alpha}| = 1{\cdot}47$; (*b*) $|\bar{\alpha}| = 2{\cdot}93$; (*c*) $|\bar{\alpha}| = 4{\cdot}40$; and (*d*) $= 8{\cdot}80$. These values were chosen the same as for the Glauber coherent states (figure 5 (*a*), (*b*), (*c*), (*f*)) for comparison. The darker a region the higher is the value of the W-function. Negative values are marked by crosses.

θ_m, respectively). If $|\bar{\alpha}|^2 \gg s/2$, the situation is the inverse: the seond term of equation (17) is now predominant and we observe two peaks for $n > s/2$ and a peak–anti-peak structure for $n \leqslant s/2$. In the case when $|\bar{\alpha}|^2 \approx s/2$, the W-function has a more general shape. With increasing $|\bar{\alpha}|$ the two-peak structure shifts to larger values of n, while the peak–anti-peak structure vanishes at $n = s$ and reappears at $n = 0$. The shape is still comparatively simple because the function (17) is a sum of only two factorizable terms.

3.2 *Glauber coherent states in FDHS*

The coherent states $|\alpha\rangle_{(s)}$ in the $(s + 1)$-dimensional Hilbert space of a harmonic oscillator can be defined in the Glauber sense by the action of the analogue of the Glauber displacement operator $\hat{D}^{(s)}(\alpha) = \exp(\alpha\hat{a}^\dagger - \alpha^*\hat{a})$ on the vacuum state, as was suggested by Bužek *et al.* [8]. The coherent states $|\alpha\rangle_{(s)}$ are the close *analogues* of usual (i.e. infinite-dimensional) Glauber coherent states $|\alpha\rangle_{(\infty)}$. They were introduced and discussed by Bužek *et al.* [8] and their general explicit form was found by Miranowicz *et al.* [9]. In Fock base, the finite-dimensional Glauber coherent state $|\alpha\rangle_{(s)}$, with $\alpha = |\alpha| \exp(i\varphi)$, is [9]

$$|\alpha\rangle_{(s)} = \hat{D}^{(s)}(\alpha)|0\rangle = \exp(\alpha\hat{a}^\dagger - \alpha^*\hat{a})|0\rangle = \sum_{n=0}^{s} \exp(in\varphi) b_n^{(s)} |n\rangle, \tag{20}$$

where

$$b_n^{(s)} = \frac{s!}{s+1}(n!)^{-1/2}(-\mathrm{i})^n \sum_{k=0}^{s} \exp(\mathrm{i}x_k|\alpha|)\mathrm{He}_n(x_k)\mathrm{He}_s^{-2}(x_k) \tag{21}$$

Here, $x_k \equiv x_k^{(s+1)}$ are the roots of the so-called modified Hermite polynomial of order $(s+1)$, $\mathrm{He}_{s+1}(x_k) = 0$, and $\mathrm{He}_n(x) \equiv 2^{-n/2}\mathrm{He}_n(x/2^{1/2})$. In figure 2 we have presented the coefficients $b_n^{(s)}$ (21) of the $(s+1)$-dimensional ($s = 1, 18$) Glauber coherent states $|\alpha\rangle_{(s)}$ in their dependence upon the parameter $|\alpha|$. The coefficients $b_n^{(s)}$ (21) for $|\alpha\rangle_{(s)}$ are periodic (for $s = 1, 2$) or quasi-periodic (for higher s) functions of $|\bar{\alpha}|$. We emphasize this essential difference between the finite-dimensional Glauber coherent states (20) and the truncated coherent states (9). Nevertheless, both $|\alpha\rangle_{(s)}$ and $|\bar{\alpha}\rangle_{(s)}$, go over into the usual (i.e. infinite-dimensional) Glauber coherent states $|\alpha\rangle_{(\infty)}$ in the limit $s \to \infty$. In order to prove this property for $|\alpha\rangle_{(s)}$ let us expand the scalar products between $|\alpha\rangle_{(s)}$ and $|\alpha\rangle_{(\infty)}$ in a series of a parameter $|\alpha|$, analogously to the expansions (12)–(15) of the truncated coherent states $|\bar{\alpha}\rangle_{(s)}$. We find the following power series for particular values of s (equal to 1, 2, 3):

$${}_{(\infty)}\langle\alpha|\alpha\rangle_{(1)} = 1 - |\alpha|/4 + |\alpha|^6/9 - \mathcal{O}(|\alpha|\alpha^8), \tag{22}$$

$${}_{(\infty)}\langle\alpha|\alpha\rangle_{(2)} = 1 - |\alpha|^6/12 + 3|\alpha|^8/64 - \mathcal{O}(|\alpha|^{10}), \tag{23}$$

$${}_{(\infty)}\langle\alpha|\alpha\rangle_{(3)} = 1 - |\alpha|^8/48 + |\alpha|^{10}/75 - \mathcal{O}(|\alpha|^{12}). \tag{24}$$

Again we see that the finite-dimensional Glauber CS $|\alpha\rangle_{(s)}$ approach the usual CS $|\alpha\rangle_{(\infty)}$ with increasing dimension in a form (15), i.e.

$${}_{(\infty)}\langle\alpha|\alpha\rangle_{(s)} = 1 - \frac{|\alpha|^{2(s+1)}}{2(s+1)!} + \mathcal{O}(|\alpha|^{2(s+2)}). \tag{25}$$

However, the states $|\alpha\rangle_{(s)}$ approach $|\alpha\rangle_{(\infty)}$ slower than $|\bar{\alpha}\rangle_{(s)}$ do, since the respective terms $\mathcal{O}(|\alpha|^{2(s+2)})$ are smaller in equations (12)–(15) than in equations (22)–(25). Finally, let us expand in a power series of $|\alpha| \equiv |\bar{\alpha}|$ the scalar products between $|\alpha\rangle_{(s)}$ and $|\bar{\alpha}\rangle_{(s)}$ for $s = 1, 2, 3$. We find for $\alpha = \bar{\alpha}$ that

$${}_{(1)}\langle\alpha|\bar{\alpha}\rangle_{(1)} = 1 - |\alpha|^6/18 + |\alpha|^8/15 - \mathcal{O}(|\alpha|^{10}), \tag{26}$$

$${}_{(2)}\langle\alpha|\bar{\alpha}\rangle_{(2)} = 1 - |\alpha|^8/64 + 9|\alpha|^{10}/800 - \mathcal{O}(|\alpha|^{12}), \tag{27}$$

$${}_{(3)}\langle\alpha|\bar{\alpha}\rangle_{(3)} = 1 - |\alpha|^{10}/300 + 13|\alpha|^{12}/5040 - \mathcal{O}(|\alpha|^{14}). \tag{28}$$

We conclude that

$${}_{(s)}\langle\alpha|\bar{\alpha}\rangle_{(s)} = 1 - \frac{|\alpha|^{2(s+2)}}{2s!(s+2)^2} + \mathcal{O}(|\alpha|^{2(s+3)}). \tag{29}$$

In figure 3, we have shown the dependence on $|\alpha| \equiv |\bar{\alpha}|$ of squared scalar products $|{}_{(s)}\langle\alpha|\bar{\alpha}\rangle_{(s)}|^2$ (solid lines), $|{}_{(\infty)}\langle\alpha|\alpha\rangle_{(s)}|^2$ (dashed) and $|{}_{(\infty)}\langle\alpha|\bar{\alpha}\rangle_{(s)}|^2$ (dash–dotted), i.e. between the usual Glauber coherent states $|\alpha\rangle_{(\infty)}$, the truncated coherent states $|\bar{\alpha}\rangle_{(s)}$ (9) and the finite-dimensional Glauber coherent states $|\alpha\rangle_{(s)}$ (20). All these states approximately equal for $|\alpha|^2 \ll s$ since the scalar products between them tend to unity. However, the states are significantly different for values $|\alpha|^2 \approx s$, becoming orthogonal for $|\alpha|^2 \gg s$. By comparison with equations (25) and (29) and as clearly shown in figure 3, we note that the finite-dimensional coherent states $|\alpha\rangle_{(s)}$ and $|\bar{\alpha}\rangle_{(s)}$ approach each other faster than the usual coherent state $|\alpha\rangle_{(\infty)}$.

On insertion of the coefficients from equation (21) into the general formula (8), we get for the states $|\alpha\rangle_{(s)}$ the expression:

$$W(n,\theta_m)=\sum_{k=0}^{M}\frac{\exp\left[\mathrm{i}(2k-M)(\theta_m-\varphi+\pi/2)\right]}{[k!(M-k)!]^{1/2}}G_{0k}+\sum_{k=M+1}^{s}\frac{\exp\left[\mathrm{i}(2k-M-s-1)(\theta_m-\varphi+\pi/2)\right]}{[k!(M-k+s+1)!]^{1/2}}G_{1k}, \tag{30}$$

where

$$G_{\eta k}\equiv G_{\eta k}^{(s)}(|\alpha|)=\frac{(s!)^2}{(s+1)^3}\sum_{p=0}^{s}\sum_{q=0}^{s}\exp\left[\mathrm{i}(x_q-x_p)|\alpha|\right]\frac{\mathrm{He}_k(x_p)\mathrm{He}_{M-k+\eta(s+1)}(x_q)}{[\mathrm{He}_s(x_p)\mathrm{He}_s(x_q)]^2} \tag{31}$$

with $\eta=0,1$. Writing equation (30) in a form more similar to the Vaccaro–Pegg expression, we arrive at

$$W(n,\theta^m)=\sum_{k=0}^{2n}(-1)^{k-n}\frac{\cos\left[(2k-2n)(\theta_m-\varphi)\right]}{[k!(2n-k)!]^{1/2}}G_{0k}+\sum_{k=2n+1}^{s}(-1)^{k-n-s/2}\frac{\sin\left[(2k-2n-s-1)(\theta_m-\varphi)\right]}{[k!(2n-k+s+1)!]^{1/2}}G_{1k} \tag{32}$$

for $n\leqslant s/2$, and

$$W(n,\theta_m)=\sum_{k=0}^{2n-s-1}(-1)^{k-n-s/2}\frac{\sin\left[(2k-2n+s+1)(\theta_m-\varphi)\right]}{[k!(2n-k-s-1)!]^{1/2}}G_{0k}+\sum_{k=2n-s}^{s}(-1)^{k-n}\frac{\cos\left[(2k-2n)(\theta_m-\varphi)\right]}{[k!(2n-k)!]^{1/2}}G_{1k} \tag{33}$$

for $n>s/2$. As readily seen, we cannot generally factorize this function into a product of amplitude $|\alpha|$ dependent and phase φ dependent parts; the behaviour of the W-functions of these states is much more complicated than in the case of truncated coherent states.

From our numerical results we note (figure 5) that for $|\alpha|^2\ll s/2$ the W-function is similar to that for truncated coherent states (figure 4). Studying the numerical results for $s=18$, we observed the following behaviour of the W-function. The shape of the respective graph is approximately periodic ('quasi-periodic') in the parameter $|\alpha|$ with quasi-period $T\approx 8{\cdot}8$. At $|\alpha|$ increasing from zero, the shape of the Glauber coherent states was initially very similar to that of the truncated coherent states (see figure 4) up to the peak–anti-peak transition from $n=s$ to $n=0$ around the value $|\alpha|\approx T/3$ (figure 5 (*b*)). Then interesting oscillations in photon number appear, culminating for $|\alpha|=T/2$ (figure 5 (*c*)), where only even photon numbers are present. For this value of α the Glauber coherent state approaches an even CS, i.e. the case of a Schrödinger cat state. Further increasing of $|\alpha|$ returns the W-function to its previous shapes through the transition regime (for $|\alpha|\approx 2T/3$—figure 5 (*d*)) to the case of the inner two-peak and outer peak–anti-peak structure, similar to the Vaccaro–Pegg results. For $|\alpha|\approx 5T/6$ (figure 5 (*e*)) the W-function graph is very similar to the $|\alpha|\approx T/6$ (figure 5 (*a*)) graph but the phase is opposite. Finally, for $|\alpha|=T$ (figure 5 (*f*)) we arrive at an almost vacuum

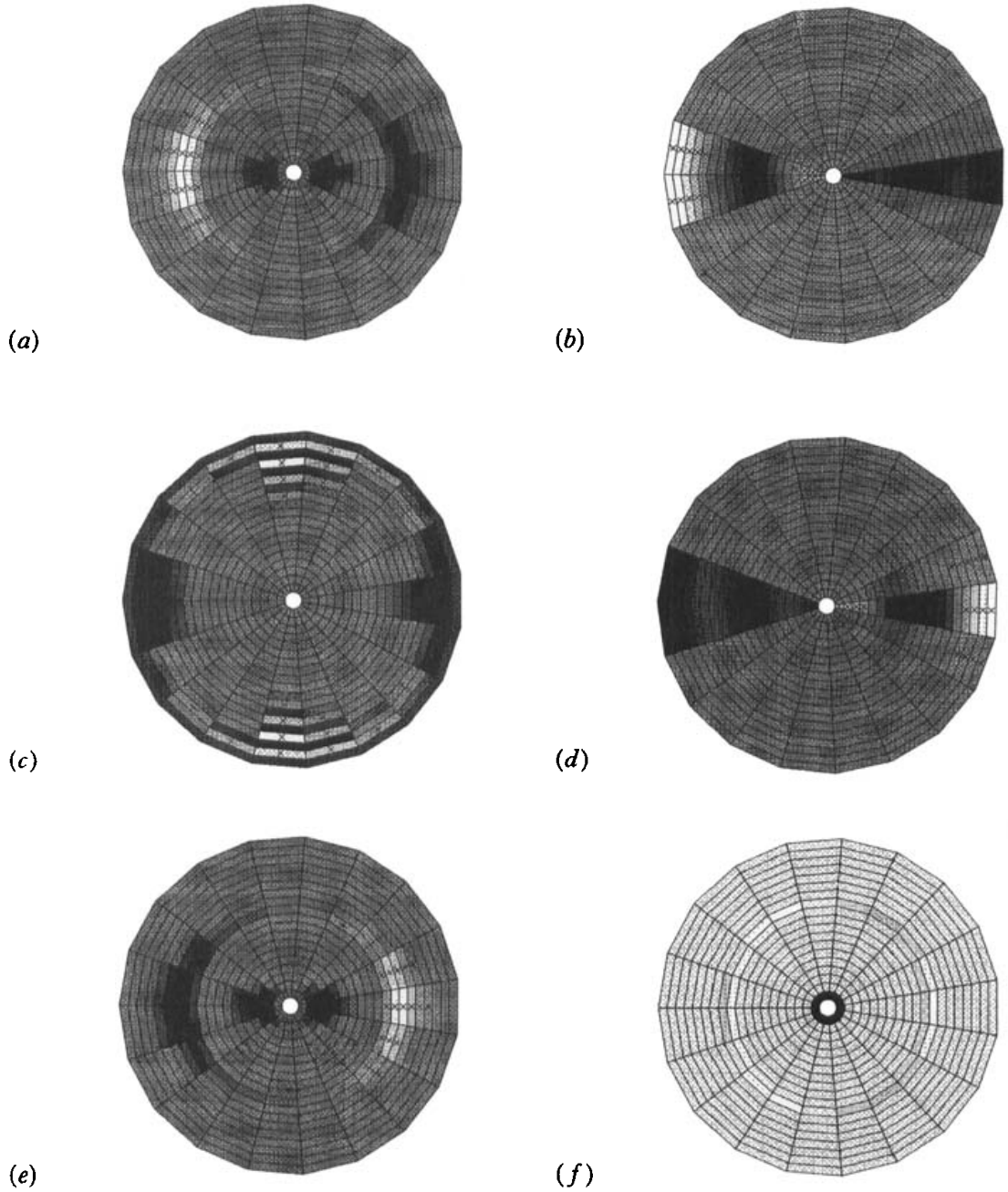

Figure 5. Wigner function of Glauber coherent states $|\alpha\rangle_{(s)}$, (20), for $s = 18$, $\alpha = |\alpha| \exp(i\varphi)$, $\varphi = 0$: (*a*) $\alpha = (1/6)T$; (*b*) $\alpha = (2/6)T$; (*c*) $\alpha = (3/6)T$; (*d*) $\alpha = (4/6)T$; (*e*) $\alpha = (5/6)T$; (*f*) $\alpha = (6/6)T$ and the quasi-period $T = 8{\cdot}8$.

state. Increasing $|\alpha|$ further, these shapes of the W-function graph reappeared for several quasi-periods T. Similar behaviour was observed also for other values of s.

This situation can be explained as follows. By applying the fitting procedure, based on the WKB method idea, we have found that the smallest positive root $x_1 \equiv x_1^{(s+1)}$ of the modified Hermite polynomial $\mathrm{He}_{s+1}(x)$ is approximately equal to

$$x_1^{(s+1)} \approx 2\pi(4s + 6)^{-1/2} \tag{34}$$

(for even s). Besides, it is well known that the nearest-to-zero roots of the Hermite polynomials are approximately equidistant. Thus, their difference $\Delta x \equiv x_{k+1} - x_k$ is approximately given by (34) which is 0·71 for $s = 18$. The predominant terms

of the sum in (21) depend upon $|\alpha|$ approximately as $\exp(ig\Delta x|\alpha|)$, where $g = 0, \pm 1, \pm 2 \ldots$. These exponential functions are periodic with approximately mean period ('quasi-period'):

$$T \approx (4s + 6)^{1/2} \tag{35}$$

for even s. By equation (35), the quasi-period for $s = 18$ is approximately 8·8. Because for n odd $\mathrm{He}_n(-x_k) = (-1)^n \mathrm{He}_n(x_k)$, the odd coefficients n in the sum (24) contain sine functions, which are zero in the middle of their period. Therefore for $|\alpha| = T/2$ the odd n terms almost disappear and we approximately get an even coherent state. We analyse in detail W-functions for even s only. Nonetheless, for completeness of our discussion we find the explicit approximate expression for the quasi-period

$$T \approx 2(4s + 6)^{1/2} \tag{36}$$

for odd s, which is twice as large as (35) for a given s.

4. Two-level coherent states and their properties

The simplest case of a finite-dimensional Hilbert space system is the two-level system, i.e. with $s = 1$. States in such a system have been intensively studied by authors dealing with the general problem (s finite) [8, 10, 11]; here we would like to discuss this problem from other points of view. Two-level systems are well known from other branches of physics, and we can thus apply the results and concepts to describe our situation. Examples of realizations of such a system can be given by the spin projection of a spin-$\frac{1}{2}$ particle, or a two-level atom. Hence, the coherent states in $\mathscr{H}^{(1)}$ (see equations (38) and (40)) can in fact be identified with the coherent spin-$\frac{1}{2}$ state [20] or equivalently with the two-level atomic coherent state [21]. In the case of $s = 1$, the terms 'photon number', 'phase' and 'finite-dimensional harmonic oscillator' are a bit confusing and should be understood, for example, as in [12]: 'z component of spin divided by $\hbar$' 'angle of orientation about the z axis' and 'spin', respectively, or equivalently as atomic quantities [21, 8]. Also, we do not use the notions *two-dimensional* space or states. This terminology could be misleading even though it is consistent with our terminology applied in former sections. In this section we shall use a Poincaré sphere representation for the description of the states discussed and their properties, like various operator averages and squeezing degrees. Finally, we present the W-function for two-level coherent states.

It is well known that states in a two-level system can be described by means of the Stokes parameters and visualized by means of the Poincaré sphere. The density matrix of any two-state system can be written in the form

$$\hat{\rho} = \frac{1}{2}\begin{pmatrix} 1 + \mathscr{S}_z & \mathscr{S}_x + i\mathscr{S}_y \\ \mathscr{S}_x - i\mathscr{S}_y & 1 - \mathscr{S}_z \end{pmatrix}, \tag{37}$$

where $\mathscr{S}_x$, $\mathscr{S}_y$ and $\mathscr{S}_z$ are the Stokes parameters. Using these parameters as coordinates of a point in three-dimensional space, any state corresponds to a point on a unit radius sphere, the so-called Poincaré sphere. Pure states are represented by points on the surface, while mixed-state points lie inside the sphere. Now, using this tool, we can display both the two-level Glauber and truncated CS and compare their expressions.

Writing for the coherent states (20)

$$|\alpha\rangle_{(1)} = \cos|\alpha||0\rangle + \exp(i\varphi)\sin|\alpha||1\rangle, \tag{38}$$

we find that the Stokes parameters are

$$\begin{aligned} \mathscr{S}_x &= \sin 2|\alpha| \cos\varphi, \\ \mathscr{S}_y &= -\sin 2|\alpha| \sin\varphi, \\ \mathscr{S}_z &= \cos 2|\alpha|. \end{aligned} \tag{39}$$

We now note that any pure state in $\mathscr{H}^{(1)}$ is coherent. The interpretation of the parameter α is very simple: its modulus is proportional to the polar coordinate, while its argument φ is the azimuthal coordinate of the representative Poincaré sphere point.

Similarly, we find the Stokes parameters for the truncated coherent states $|\bar{\alpha}\rangle_{(1)}$ (9). The two-level state $|\bar{\alpha}\rangle_{(1)}$, with the parameter $\bar{\alpha} = |\bar{\alpha}|\exp(i\varphi)$, is expressed by

$$\begin{aligned} |\bar{\alpha}\rangle_{(1)} &= \frac{1}{(1+|\bar{\alpha}|^2)^{1/2}}|0\rangle + \exp(i\varphi)\frac{|\bar{\alpha}|}{(1+|\bar{\alpha}|^2)^{1/2}}|1\rangle \\ &= \cos(\arctan|\bar{\alpha}|)|0\rangle + \exp(i\varphi)\sin(\arctan|\bar{\alpha}|)|1\rangle. \end{aligned} \tag{40}$$

The Stokes parameters are now

$$\begin{aligned} \mathscr{S}_x &= 2\frac{|\bar{\alpha}|}{1+|\bar{\alpha}|^2}\cos\varphi, \\ \mathscr{S}_y &= -2\frac{|\bar{\alpha}|}{1+|\bar{\alpha}|^2}\sin\varphi, \\ \mathscr{S} &= \frac{1-|\bar{\alpha}|^2}{1+|\bar{\alpha}|^2}. \end{aligned} \tag{41}$$

The function of the argument φ is the same as for the Glauber coherent state (38), while the modulus $|\bar{\alpha}|$ has a different meaning to $|\alpha|$ (we observe, for example, that there is neither periodicity nor quasi-periodicity in $|\bar{\alpha}|$). To interpret $|\bar{\alpha}|$, we write the last equation in (41) in the form $|\bar{\alpha}|/(1-\mathscr{S}_z^2)^{1/2} = 1/(1+\mathscr{S}_z)$. Thus, for a given $\bar{\alpha}$, we can construct the corresponding Poincaré sphere point in the following way (see figure 6): first we locate the complex number $\bar{\alpha}$ in the $\mathscr{S}_x\mathscr{S}_y$ plane so that

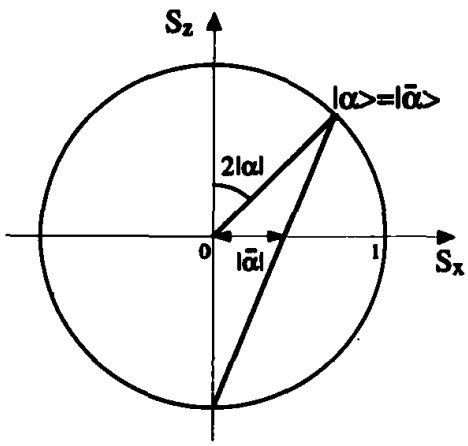

Figure 6. Poincaré sphere representation of a two-level Glauber coherent state $|\alpha\rangle_{(1)}$ and truncated coherent state $|\bar{\alpha}|_{(1)}$. For simplicity, φ was chosen as zero.

the $\mathscr{S}_x$ ($-\mathscr{S}_y$) coordinate is the real (imaginary) part of $\bar{\alpha}$, respectively. We now connect this point with the lower pole of the Poincaré sphere by a straight line; the other intersection of the line and the sphere is then the point representing the coherent state.

For the case of two-level coherent states, quantities have been computed like the mean values and variances of the various operators, including $\hat{N}$, $\hat{\Phi}_\theta$, quadratures, their commutators, etc. [8, 10]. Most of these quantities can be easily displayed on the Poincaré sphere and expressed by means of the Stokes parameters. We find that the following mean values and variances are given respectively by (see figure 7 (*a*))

$$\begin{aligned} \langle \hat{N} \rangle &= (1 - \mathscr{S}_z)/2, \\ \langle (\Delta \hat{N})^2 \rangle &= (\mathscr{S}_x^2 + \mathscr{S}_y^2)/4, \\ \langle \hat{\Phi}_\theta \rangle &= (1 - \mathscr{S}_x)\pi/2, \\ \langle (\Delta \hat{\Phi}_\theta)^2 \rangle &= (\mathscr{S}_y^2 + \mathscr{S}_z^2)\pi^2/4, \end{aligned} \tag{42}$$

and the mean value of the $\hat{N} - \hat{\Phi}_\theta$ commutator is

$$\langle [\hat{N}, \hat{\Phi}_\theta] \rangle = i\pi \mathscr{S}_y/2. \tag{43}$$

The degrees of squeezing S_N and S_Φ defined by

$$\begin{aligned} S_N &= \frac{2\langle (\Delta \hat{N})^2 \rangle - |\langle [\hat{N}, \hat{\Phi}_\theta] \rangle|}{|\langle [\hat{N}, \hat{\Phi}_\theta] \rangle|}, \\ S_\Phi &= \frac{2\langle (\Delta \hat{\Phi}_\theta)^2 \rangle - |\langle [\hat{N}, \hat{\Phi}_\theta] \rangle|}{|\langle [\hat{N}, \hat{\Phi}_\theta] \rangle|}, \end{aligned} \tag{44}$$

can be written in terms of the Stokes parameters by (see figure 7 (*b*))

$$\begin{aligned} S_N &= \frac{1}{\pi} \frac{\mathscr{S}_x^2 + \mathscr{S}_y^2}{|\mathscr{S}_y|} - 1, \\ S_\Phi &= \pi \frac{\mathscr{S}_y^2 + \mathscr{S}_z^2}{|\mathscr{S}_y|} - 1. \end{aligned} \tag{45}$$

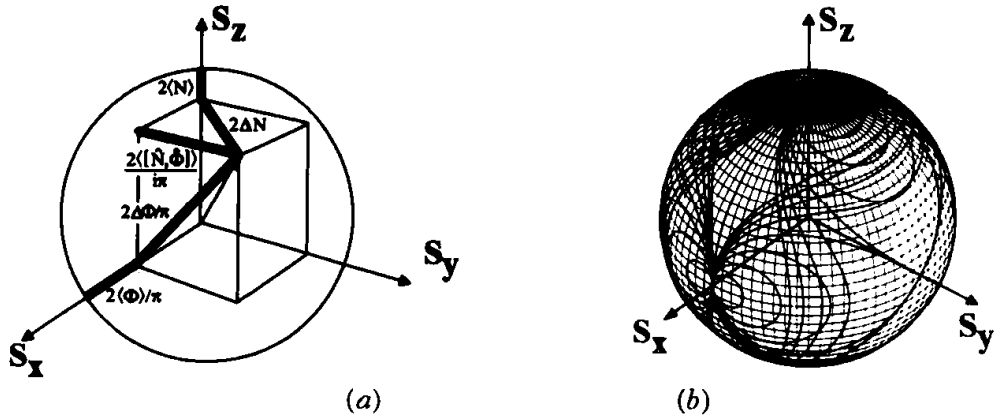

Figure 7. Poincaré sphere representation of the mean values, uncertainties of $\hat{N}$ and $\hat{\Phi}_\theta$ and mean commutator (*a*) and squeezings (*b*). Here $\Delta N \equiv (\langle (\Delta \hat{N})^2 \rangle)^{1/2}$, and similarly for $\Delta\Phi$. The lines of constant squeezing S_N in (*b*) emerge from the poles $\mathscr{S}_z = \pm 1$ and those of constant phase squeezing S_Φ emerge from the equatorial points $\mathscr{S}_x = \pm 1$.

We found that in the case $s = 1$, the averages of the quantum optical quantities are simply related to the Stokes parameters. The correspondence can also be expressed in terms of operators—$\hat{N}$ and $\hat{\Phi}_\theta$ are related to the Pauli matrices $\hat{\sigma}_z$ and $\hat{\sigma}_x$, the quadratures $\hat{X}_a$ and $\hat{Y}_a$ to the matrices $\hat{\sigma}_x$ and $\hat{\sigma}_y$.

Finally, we also find the explicit expression for the Wigner function in n and θ for these two-level states. Expressing the mean values for the phase space point operators (4) in the Glauber coherent state $|\alpha\rangle_{(1)}$, (20), we get the W-function

$$W(n, \theta_m) = (1/4)[1 + (-1)^n \cos(2|\alpha|) + (-1)^m 2^{1/2} \sin(2|\alpha|) \cos(\varphi - (-1)^n \pi/4)]. \quad (46)$$

If we simply substitute $\arctan|\bar{\alpha}|$ instead of $|\alpha|$ into (46), we obtain the W-function for the truncated coherent states $|\alpha\rangle_{(1)}$, (9).

5. Concluding remarks

The expression of different finite-dimensional coherent states by quasi-distributions enables a very intuitive understanding of some of their properties. Here, we have tried to propose graphical representations of W-functions for finite-dimensional coherent states, often discussed in recent works. We have compared the $(s + 1)$-dimensional Glauber coherent states $|\alpha\rangle_{(s)}$ (defined by the action of the generalized finite-dimensional displacement operator on vacuum) with the truncated coherent states $|\bar{\alpha}\rangle_{(s)}$ (defined by the normallized truncated Fock expansion of the usual Glauber coherent states $|\alpha\rangle_{(\infty)}$). We have shown both analytically and graphically that these coherent states constructed in finite-dimensional Hilbert spaces $\mathcal{H}^{(s)}$ exhibit essentially different behaviour: the states $|\alpha\rangle_{(s)}$ are periodic (for $s = 1, 2$) or quasi-periodic (for higher $s < \infty$) functions of the parameter $|\alpha|$, whereas the truncated states $|\bar{\alpha}\rangle_{(s)}$ are aperiodic in $|\bar{\alpha}|$ for any s (even for $s = 1$). Both $|\alpha\rangle_{(s)}$ and $|\bar{\alpha}\rangle_{(s)}$ go over into the usual coherent states $|\alpha\rangle_{(\infty)}$ in the limit of $s \to \infty$, nevertheless, the states $|\bar{\alpha}\rangle_{(s)}$ approach $|\alpha\rangle_{(\infty)}$ faster than the $|\alpha\rangle_{(s)}$ do. Besides, as a special case, we have compared in detail the two-level coherent states. There are numerous other interesting finite-dimensional states (like Schrödinger cats, displaced number states, phase coherent states, etc.) which deserve deeper study of their properties represented by quasi-distributions. We shall study them elsewhere [22].

The numerical computations were performed using MATHEMATICA (processing analytical expressions, like equation (21), etc.) and MATLAB (for direct use of the displacement operator as an exponential of matrices and for generating the W-function graphs).

Acknowledgements

We are grateful to J. Peřina, R. Tanaś and K. Piątek for their valuable comments. One of us (A.M.) has also benefited greatly from his contact with S. M. Barnett, V. Bužek, K. Flatau, P. L. Knight, G. Kurizki and Yu. P. Malakyan. This work was carried out within the framework of Project 2 PO3B 188 8 of the Polish State Committee for Scientific Research and was supported in part by the Czech Academy of Sciences and by an internal grant from the Palacký University 31403003-IG.

References

[1] KLAUDER, J. R., and SKAGERSTAM, B. S. (editors), 1985, *Coherent states: Applications in Physics and Mathematical Physics* (Singapore: World Scientific); PERELOMOV, A. M., 1986, *Gemeralized Coherent States and their Applications* (Berlin: Springer-Verlag); ZHANG, W. M., FENG, D. H., and GILMORE, R., 1990, *Rev. mod. Phys.*, **62,** 867.

[2] PEGG, D. T., and BARNETT, S. M., 1988, *Europhys. Lett.*, **6,** 483; 1989, *Phys. Rev.* A, **41,** 3427; BARNETT, S. M., and PEGG, D. T., 1989, *J. mod. Optics*, **36,** 7.

[3] BUŽEK, V., WILSON-GORDON, A. D., KNIGHT, P. L., and LAI, W. K., 1992, *Phys. Rev.* A, **45,** 8079.

[4] VOGEL, K., AKULIN, V. M., and SCHLEICH, W. P., 1993, *Phys. Rev. Lett.*, **71,** 1816.

[5] GARRAWAY, B. M., SHERMAN, B., MOYA-CESSA, H., KNIGHT, P. L., and KURIZKI, G., 1994, *Phys. Rev.* A, **49,** 535.

[6] LEOŃSKI, W., and TANAŚ, R., 1994, *Phys. Rev.* A, **49,** R20.

[7] PEŘINA, J., HRADIL, Z., and JURČO, B., 1994, *Quantum Optics and Fundamentals of Physics*, volume 63 of *Fundamental Theories in Physics* (Dordrecht: Kluwer Acad.).

[8] GLAUBER, R. J., 1963, *Phys. Rev.*, **131,** 2766.

[9] MIRANOWICZ, A., PIĄTEK, K., and TANAŚ, R., 1994, *Phys. Rev.* A, **50,** 3423.

[10] KUANG, L. M., WANG, F. B., and ZHOU, Y. G., 1994, *Phys. Lett.* A, **183,** 1; 1993, *J. mod. Optics.*, **42,** 1307.

[11] GANGOPADHYAY, G., 1994, *J. mod. Optics*, **41,** 525; ZHU, J. Y., and KUANG, L. M., 1994, *Phys. Lett.* A, **193,** 227; KUANG, L. M., and CHEN, X., 1994, *Phys. Rev.* A, **50,** 4228; *Idem* 1994, *Phys. Lett.* A, **186,** 8.

[12] WOOTTERS, W. K., 1987, *Ann. Phys.*, **176,** 1.

[13] VACCARO, J. A., and PEGG, D. T., 1990, *Phys. Rev.* A, **41,** 5156.

[14] HILLERY, M., O'CONNELL, R. F., SCULLY, M. O., and WIGNER, E. P., 1984, *Phys. Rep.*, **106,** 121; TATARSKII, V. I., 1983, *Sov. Phys. Usp.*, **26,** 311.

[15] STRATONOVICH, R. L., 1957, *Sov. Phys. JETP*, **4,** 891; O'CONNEL, R. F., and WIGNER, E. P., 1984, *Phys. Rev.* A, **30,** 2613; COHEN, L., and SCULLY, M. O., 1986, *Found. Phys.*, **16,** 295.

[16] GALETTI, D., and DE TOLEDO-PIZA, A. F. R., 1988, *Physica* A, **149,** 267.

[17] LUKŠ, A., and PEŘINOVÁ, V., 1993, **T48,** 94.

[18] VACCARO, J. A., 1995, *Optics Commun.*, **113,** 421.

[19] Vaccaro and Pegg [13] claim that equation (3) holds for all odd numbers $(s + 1)$ as well.

[20] RADCLIFFE, J. M., 1971, *J. Phys.* A, **4,** 313.

[21] ARECCHI, C., COURTENS, E., GILMORE, R., and THOMAS, H., 1972, *Phys. Rev.* A, **6,** 2211.

[22] MIRANOWICZ, A., OPATRNÝ, T., and BAJER, J. (unpublished).